Research in Astron. Astrophys. **2009** Vol. **9** No. **4**, 431–448
http://www.raa-journal.org *http://www.iop.org/journals/raa*

***R**esearch in*
***A**stronomy and*
***A**strophysics*

Abundance analysis of Barium stars *

Guo-Qing Liu[1,2], Yan-Chun Liang[1] and Li-Cai Deng[1]

[1] National Astronomical Observatories, Chinese Academy of Sciences, Beijing 100012, China; *lgq@bao.ac.cn, ycliang@bao.ac.cn*
[2] Graduate University of Chinese Academy of Sciences, Beijing 100049, China

Received 2008 March 31; accepted 2008 June 17

Abstract We obtain the chemical abundances of six barium stars and two CH subgiant stars based on the high signal-to-noise ratio and high resolution Echelle spectra. The neutron capture process elements Y, Zr, Ba, La and Eu show obvious overabundances relative to the Sun, for example, their [Ba/Fe] values are from 0.45 to 1.27. Other elements, including Na, Mg, Al, Si, Ca, Sc, Ti, V, Cr, Mn and Ni, show comparable abundances to the Solar ones, and their [Fe/H] covers a range from -0.40 to 0.21, which means they belong to the Galactic disk. The predictions of the theoretical model of wind accretion for binary systems can explain the observed abundance patterns of the neutron capture process elements in these stars, which means that their overabundant heavy-elements could be caused by accreting the ejecta of AGB stars, the progenitors of present-day white dwarf companions in binary systems.

Key words: stars: abundances — stars: atmospheres — stars: chemically peculiar — stars: evolution — binaries: spectroscopic

1 INTRODUCTION

As first identified by Bidelman & Keeman (1951), barium stars appear as a distinct group of chemically peculiar red giants. These G and K giants show enhanced features of Ba II, Sr II, CH, CN and sometimes C_2 lines. The following studies also found enhanced abundances of some other heavy elements, e.g. Y, Zr, La, Ce, Pr, Nd and Sm.

Since Burbidge et al. (1957) suggested that elements heavier than iron are synthesized in the interiors of asymptotic giant branch (AGB) stars through the slow neutron capture process (s-process) (the rapid neutron capture process, r-process, occurs in supernova explosions), researchers generally believe that the overabundant heavy elements of Ba stars could be caused by binary accretion because they could not be evolved to the thermal pulse (TP) AGB stage to synthesize these heavy elements due to their low luminosity and the absence of the unstable nucleus ^{99}Tc ($\tau_{\frac{1}{2}}$=2×10^5yr) (see Liang et al. 2000, 2003 and references therein). The binarity and heavy-element abundances of Ba stars have been studied by many researchers (Griffin 1980; Jorissen & Mayor 1988; McClure et al. 1980; McClure 1983; McClure & Woodsworth 1990; Jorissen et al. 1998; Liang et al. 2000, 2003; Liu et al. 2000; Lü et al. 1991; Han et al. 1995; Začs 1994; Smiljanic et al. 2007). These Ba stars could have accreted the matter ejected by their companions (former AGB stars, present-day white dwarfs) about 1×10^6 yr ago through wind accretion, disk accretion or common envelope ejection (Han et al. 1995; Jorissen et al. 1998; Liang et al. 2000).

∗ Supported by the National Natural Science Foundation of China.

At present, a large sample of Ba stars have been studied, including their binary orbital elements (Carquillat et al. 1998; Udry et al. 1998; Jorissen et al. 1998), absolute magnitudes and kinematics (Gómez et al. 1997; Mennessier et al. 1997). However, the corresponding heavy-element abundances have not been obtained from high resolution observations, which are very useful for understanding the formation scenario of Ba stars, but need lots of telescope time and lots of effort in data analysis. Therefore, we propose observing the high resolution and high signal-to-noise (S/N) ratio spectra of a sample of Ba stars to obtain their chemical abundances. This will help us to understand their formation scenario by combining these properties with their binary orbital elements. Moreover, by taking advantage of the present high precision Hipparcos data, precise photometric parameters, improved methods for determining stellar atmospheric parameters and developing stellar evolutionary tracks etc., the reliable chemical abundances of stars could be obtained from the spectra. We could also understand the formation scenario of Ba stars from theoretical models by comparing the model predictions with the observed abundances, e.g. the angular momentum conservation model of wind accretion of Ba binaries (Liang et al. 2000; Liu et al. 2000; Boffin & Jorissen 1998).

This paper is organized as follows. Descriptions of the spectral observations and data reduction for the sample stars are presented in Section 2. In Section 3, the derived stellar atmospheric parameters are presented. Stellar atmosphere model, spectral lines and their measured equivalent widths (EWs) are described in Section 4. The analysis of abundance results is given in Section 5. The predicted abundances from the wind accretion model are presented and compared with the observed abundance patterns in Section 6. The discussion and conclusions are given in Section 7.

2 OBSERVATIONS AND DATA REDUCTION

The sample stars were first identified as mild or strong Ba stars in Lü et al. (1991) and their binary orbital elements have been obtained (e.g. orbital period and eccentricity) in Jorissen et al. (1998) except HD 4395. HD 4395 and HD 216219 were classified as CH subgiants (Luck & Bond 1982; Sneden 1983; Krishnaswamy & Sneden 1985; Lambert et al. 1993; Smith et al. 1993; Preston & Sneden 2001). HD 216219 has also been classified as a mild Ba star by Lü et al. (1991) and Jorissen et al. (1998). A common point of view is that CH subgiants also belong to binary systems and their overabundances of s-process elements are caused by accreting the ejected material of the companion AGB progenitors, which is the same scenario as the Ba stars. The CH subgiants could evolve to be the classical Ba stars (Luck & Bond 1982; Smith et al. 1993). In this work, we deal with these two stars using the same method as for other Ba star samples to study their abundances and formation scenario. These two stars have also been studied by Smith et al. (1993). Thus, they are good examples for carefully comparing our EW measurements, atomospheric parameters and abundances with theirs.

Table 1 presents the basic parameters of the sample stars. The columns (1)–(6) present their HD identifications, spectral types and luminosity classes, visual magnitudes, $B-V$ color indices, trigonometric parallaxes and the corresponding errors taken from the SIMBAD database.

Table 1 Basic Data about the Sample Stars

HD	Sp.	$V_{\rm mag}$	$B-V$	π (mas)	σ_π
4395	G5	7.70	0.69	9.16	1.12
180622	K2	7.63	1.25	3.37	1.04
201657	K2	8.00	1.27	4.49	1.07
201824	K0	8.90	1.09	0.56	1.56
210946	K0	8.08	1.095	3.42	1.14
211594	K0	8.05	1.143	4.59	1.18
216219	G0IIp	7.44	0.64	10.74	0.93
223617	G5	6.91	1.155	4.61	0.95

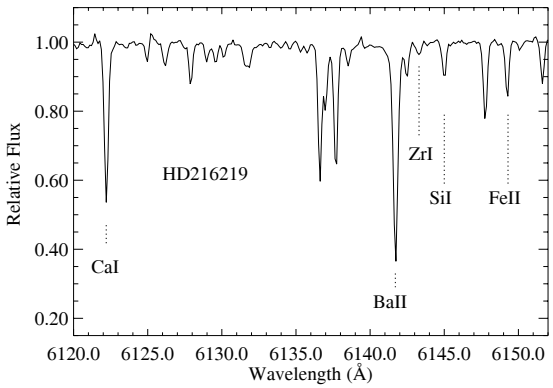

Fig. 1 A portion of the spectrum of the sample star HD 216219 in the wavelength range 6120Å−6152Å. Major features include Ca I 6122.226 Å, Ba II 6141.727 Å, Zr I 6143.180 Å, Si I 6145.020 Å and Fe II 6149.249 Å.

The spectroscopic observations were carried out with the Coudé Echelle Spectrograph of National Astronomical Observatories (NAOC) mounted on the 2.16 m telescope at Xinglong station (Xinglong, P. R. China). The detector was a Tektronix CCD with 1024×1024 pixels (each 24×24 μm^2 in size). The wavelength coverage of the total spectra is roughly from 5500−8000 Å over 34 orders. The spectra were observed during September 12−14, 2000 and most of them had S/N >100. Figure 1 presents the spectrum of HD 216219 showing main features of absorption in the region around the Ba II λ6141.727 line.

Data reduction of all the spectra was carried out through the ECHELLE package in the MIDAS environment by standard routines proceeding with order identification, background subtraction, flat-field correction, order extraction and wavelength calibration with a thorium-argon lamp calibration frame. Bias, dark current and scattered light corrections were taken into account in the background subtraction. The pixel-to-pixel sensitivity variations were corrected by using the flat-field. The EWs of the spectral lines are measured from the normalized spectra corrected by radial velocity, which were measured from more than 20 absorption lines. The selected spectral lines for abundance analysis are unblended or slightly blended and have reliable atomic data.

The EWs of the spectral lines were measured by applying two different methods: direct integration of the line profile and Gaussian fitting. The latter is preferable in the case of faint lines (EW<20 m Å), but unsuitable for the strong lines in which the damping wings contribute significantly to the equivalent widths. The final EWs are weighted averages of these two measurements, depending on the line intensity (see Zhao et al. 2000 for details). The EW values of 110−180 lines in the wavelength range from 5500−8100 Å were obtained for each of the sample stars. Table 2 presents the final EWs of the lines measured in the spectra of the sample stars as input data for the abundance analysis. Since the very weak lines would lead to an increase of random errors in the abundance determination and too strong lines are not so sensitive to abundance, we use the lines with EWs=$10 - 200$ m Å for abundance analysis, and most of them within $20 - 150$ m Å , except for some of the s-process elements. The reliability of our EW measurements has been confirmed by the consistency in the comparison between our data and those of Smith et al. (1993) for 35 common lines of HD 216219 and HD 4395. This comparison is shown in Figure 2.

The systematic difference between the two sets of data is small and could be given by a linear least square fit as:

$$\mathrm{EW}_{\mathrm{Smith93}} = 0.92(\pm 0.02)\mathrm{EW}_{\mathrm{this\ work}} + 2.19(\pm 1.30)\,\mathrm{m\AA}, \quad (1)$$

with a standard deviation of 0.061.

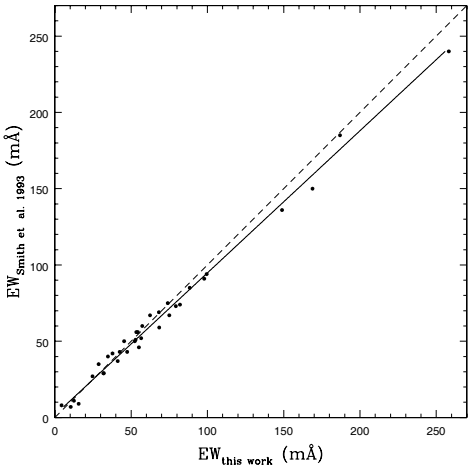

Fig. 2 Comparison of equivalent width measurements of 35 common absorption lines in HD 216219 and HD 4395 in this work and Smith et al. (1993). The solid line is the least square fit to the points (Eq. (1)), and the dashed line refers to the one-to-one relation.

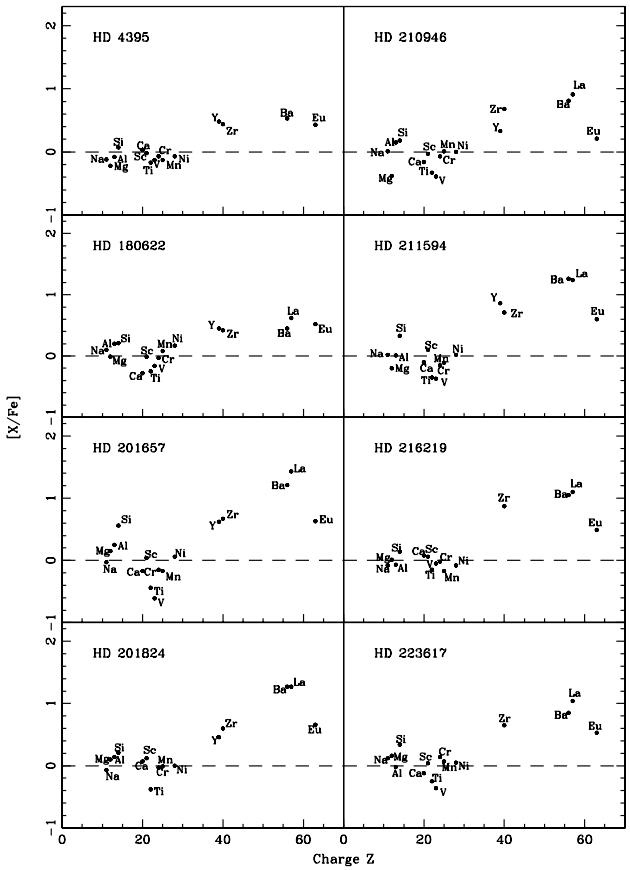

Fig. 3 The abundance patterns of sample stars.

Table 2. Equivalent Widths and Abundances for All the Sample Stars

λ (Å)	Ion	χ	log gf	Ref.	HD 4395		HD 180622		HD 201657		HD 201824		HD 210946		HD 211594		HD 216219		HD 223617	
					EW	log ϵ	EW	log ϵ	EW	log ϵ	EW	log ϵ	EW	log ϵ	EW	log ϵ	EW	log ϵ	EW	log ϵ
5522.454	Fe I	4.21	−1.55	nd	38.1	7.281	99.3	7.916	73.9	7.231	–	–	76.1	7.385	88.6	7.600	–	–	84.4	7.575
5525.552	Fe I	4.23	−1.08	cn	–	–	–	–	87.0	7.025	–	–	–	–	–	–	–	–	–	–
5543.944	Fe I	4.22	−1.14	nd	69.5	7.490	–	–	–	–	–	–	–	–	93.5	7.293	51.5	7.194	–	–
5546.514	Fe I	4.37	−1.31	nd	49.9	7.431	–	–	–	–	–	–	74.6	7.310	82.0	7.430	–	–	–	–
5560.220	Fe I	4.43	−1.19	nd	–	–	86.2	7.561	62.0	6.942	–	–	65.3	7.093	57.9	6.947	39.2	7.218	72.5	7.249
5618.642	Fe I	4.21	−1.28	cn	57.2	7.371	99.6	7.638	73.2	6.940	–	–	77.2	7.123	–	–	39.5	7.088	–	–
5633.953	Fe I	4.99	−0.27	nd	–	–	–	–	95.5	7.302	–	–	79.8	7.091	–	–	56.6	7.152	–	–
5638.271	Fe I	4.22	−0.87	nd	–	–	–	–	–	–	–	–	97.6	7.113	–	–	67.0	7.208	97.3	7.154
5641.448	Fe I	4.26	−1.18	nd	–	–	–	–	99.3	7.379	89.2	7.256	–	–	91.5	7.336	45.2	7.150	–	–
5646.686	Fe I	4.26	−2.51	nd	–	–	37.9	7.740	18.8	7.191	16.0	7.093	16.1	7.205	–	–	–	–	–	–
5651.470	Fe I	4.47	−2.00	nd	–	–	52.0	7.763	–	–	–	–	–	–	44.7	7.572	–	–	–	–
5655.183	Fe I	5.06	−0.64	nd	–	–	–	–	–	–	–	–	–	–	79.8	7.533	–	–	–	–
5662.524	Fe I	4.18	−0.57	cn	–	–	–	–	–	–	–	–	–	–	–	–	87.2	7.246	–	–
5679.032	Fe I	4.65	−0.92	nd	–	–	–	–	71.5	7.113	–	–	76.4	7.280	71.5	7.182	–	–	82.8	7.436
5705.473	Fe I	4.30	−1.36	cn	38.8	7.181	84.7	7.524	60.1	6.904	–	–	66.2	7.109	–	–	–	–	70.2	7.200
5717.841	Fe I	4.28	−1.13	nd	–	–	–	–	–	–	93.1	7.302	–	–	–	–	–	–	–	–
5731.772	Fe I	4.26	−1.30	nd	–	–	–	–	–	–	83.5	7.250	–	–	98.4	7.579	–	–	94.3	7.564
5753.132	Fe I	4.26	−0.76	nd	–	–	–	–	–	–	–	–	–	–	–	–	76.4	7.306	–	–
5775.088	Fe I	4.22	−1.17	cn	63.3	7.380	–	–	78.6	6.931	77.6	6.945	78.4	7.037	70.9	6.885	40.9	7.006	85.9	7.210
5806.732	Fe I	4.61	−1.05	lz	–	–	94.3	7.786	68.8	7.143	–	–	76.1	7.350	66.4	7.167	–	–	79.7	7.451
5809.224	Fe I	3.88	−1.84	lz	–	–	–	–	93.6	7.432	68.6	7.020	87.0	7.451	84.9	7.390	37.6	7.275	96.2	7.663
5811.917	Fe I	4.14	−2.43	nd	–	–	45.2	7.647	22.0	7.045	–	–	29.7	7.322	–	–	–	–	–	–
5845.270	Fe I	5.03	−1.82	nd	–	–	24.5	7.689	–	–	–	–	13.2	7.316	–	–	–	–	–	–
5849.682	Fe I	3.69	−2.99	nd	–	–	54.9	7.825	–	–	–	–	–	–	–	–	–	–	–	–
5852.228	Fe I	4.55	−1.33	nd	–	–	–	–	59.2	7.180	42.7	6.866	67.4	7.400	–	–	–	–	82.7	7.712
5856.096	Fe I	4.29	−1.33	ow	–	–	83.6	7.452	70.4	7.037	–	–	–	–	–	–	30.6	7.028	72.5	7.195
5858.779	Fe I	4.30	−2.26	nd	–	–	–	–	40.7	7.467	–	–	–	–	–	–	–	–	–	–
5859.596	Fe I	4.55	−0.66	lz	–	–	–	–	–	–	–	–	–	–	–	–	71.9	7.394	–	–
5862.368	Fe I	4.55	−0.45	lz	–	–	–	–	94.1	6.912	–	–	–	–	87.6	6.871	70.3	7.155	–	–
5905.680	Fe I	4.65	−0.73	lz	–	–	–	–	71.2	6.914	–	–	–	–	66.7	6.897	49.9	7.160	75.6	7.096
5927.797	Fe I	4.65	−1.09	lz	–	–	81.3	7.617	50.0	6.906	–	–	–	–	45.6	6.884	37.7	7.290	–	–
5929.682	Fe I	4.55	−1.41	lz	–	–	–	–	59.8	7.269	57.3	7.206	56.4	7.283	60.7	7.349	–	–	63.5	7.426
5930.191	Fe I	4.65	−0.23	lz	–	–	–	–	–	–	–	–	–	–	–	–	75.0	7.110	–	–
5934.665	Fe I	3.93	−1.17	lz	77.2	7.352	–	–	–	–	–	–	–	–	–	–	56.9	7.013	–	–
5952.726	Fe I	3.98	−1.44	nd	–	–	–	–	–	–	–	–	–	–	81.0	7.033	–	–	–	–
6003.022	Fe I	3.88	−1.12	lz	90.4	7.497	–	–	–	–	–	–	–	–	–	–	71.6	7.185	–	–
6024.068	Fe I	4.55	−0.12	nd	–	–	–	–	–	–	–	–	–	–	–	–	93.6	7.224	–	–
6027.059	Fe I	4.07	−1.09	cn	67.0	7.208	–	–	–	–	–	–	94.8	7.062	91.9	6.991	–	–	98.0	7.165
6034.033	Fe I	4.31	−2.42	nd	–	–	45.2	7.847	–	–	–	–	–	–	–	–	–	–	–	–
6056.013	Fe I	4.73	−0.46	lz	71.6	7.316	–	–	88.8	7.044	89.7	7.088	90.0	7.141	80.8	6.969	64.3	7.221	94.5	7.275
6079.016	Fe I	4.65	−1.12	lz	–	–	86.8	7.746	68.6	7.251	–	–	73.3	7.404	66.5	7.278	–	–	77.2	7.507
6093.649	Fe I	4.61	−1.50	lz	26.2	7.355	71.6	7.787	49.4	7.248	38.6	7.022	50.9	7.344	45.9	7.247	–	–	58.9	7.500
6094.370	Fe I	4.65	−1.94	nd	–	–	–	–	–	–	–	–	–	–	32.1	7.472	–	–	–	–
6096.671	Fe I	3.98	−1.93	lz	41.9	7.471	83.1	7.638	62.4	7.091	–	–	65.7	7.263	54.4	7.051	23.1	7.136	69.9	7.350
6105.150	Fe I	4.55	−2.07	nd	–	–	–	–	–	–	–	–	32.2	7.492	–	–	–	–	–	–
6137.002	Fe I	2.20	−2.87	cn	–	–	–	–	–	–	–	–	–	–	–	–	77.0	7.304	–	–
6151.623	Fe I	2.18	−3.28	cn	56.6	7.213	–	–	–	–	–	–	–	–	–	–	–	–	–	–
6157.733	Fe I	4.07	−1.26	nd	–	–	–	–	–	–	–	–	–	–	–	–	62.4	7.334	–	–
6159.370	Fe I	4.61	−1.97	nd	–	–	–	–	37.2	7.494	28.7	7.288	–	–	42.0	7.643	–	–	–	–
6165.363	Fe I	4.14	−1.47	cn	42.5	7.187	98.5	7.682	82.3	7.180	–	–	80.5	7.259	71.6	7.086	–	–	82.9	7.331
6173.341	Fe I	2.22	−2.88	cn	79.3	7.301	–	–	–	–	–	–	–	–	–	–	–	–	–	–
6180.209	Fe I	2.73	−2.58	cn	68.4	7.327	–	–	–	–	–	–	–	–	–	–	47.4	7.013	–	–
6187.995	Fe I	3.94	−1.72	cn	55.8	7.482	97.8	7.657	84.8	7.208	75.1	7.066	70.1	7.074	83.5	7.294	–	–	86.8	7.401
6200.321	Fe I	2.61	−2.44	cn	74.4	7.172	–	–	–	–	–	–	–	–	–	–	64.5	7.059	–	–

Table 2 (continued)

λ (Å)	Ion	χ	log gf	Ref.	HD 4395		HD 180622		HD 201657		HD 201824		HD 210946		HD 211594		HD 216219		HD 223617	
					EW	log ϵ	EW	log ϵ	EW	log ϵ	EW	log ϵ	EW	log ϵ	EW	log ϵ	EW	log ϵ	EW	log ϵ
6213.437	Fe I	2.22	−2.58	nd	89.2	7.197	–	–	–	–	–	–	–	–	–	–	–	–	–	–
6215.149	Fe I	4.19	−1.13	lz	76.9	7.551	–	–	–	–	91.9	7.117	–	–	–	–	44.8	7.002	–	–
6229.232	Fe I	2.84	−2.81	cn	42.7	7.168	–	–	–	–	–	–	86.5	7.065	–	–	–	–	99.2	7.313
6232.648	Fe I	3.65	−1.22	cn	91.0	7.365	–	–	–	–	–	–	–	–	–	–	77.0	7.154	–	–
6240.653	Fe I	2.22	−3.27	cn	70.9	7.514	–	–	–	–	–	–	–	–	–	–	43.9	7.099	–	–
6246.327	Fe I	3.60	−0.88	cn	–	–	–	–	–	–	–	–	–	–	–	–	94.2	7.104	–	–
6270.231	Fe I	2.86	−2.61	cn	63.1	7.377	–	–	–	–	–	–	–	–	–	–	50.1	7.220	–	–
6301.508	Fe I	3.65	−0.72	cn	–	–	–	–	–	–	–	–	–	–	–	–	95.5	6.972	–	–
6330.852	Fe I	4.73	−1.74	nd	–	–	–	–	–	–	–	–	–	–	49.1	7.683	–	–	–	–
6336.830	Fe I	3.69	−0.86	cn	–	–	–	–	–	–	–	–	–	–	–	–	85.8	6.969	–	–
6344.155	Fe I	2.43	−2.90	cn	–	–	–	–	–	–	–	–	–	–	–	–	68.2	7.379	–	–
6358.687	Fe I	0.86	−4.17	cn	90.6	7.299	–	–	–	–	–	–	–	–	–	–	–	–	–	–
6380.750	Fe I	4.19	−1.29	cn	59.8	7.375	–	–	–	–	–	–	97.5	7.431	85.2	7.195	39.2	7.036	–	–
6408.026	Fe I	3.69	−1.01	cn	–	–	–	–	–	–	–	–	–	–	–	–	88.4	7.165	–	–
6419.956	Fe I	4.73	−0.24	nd	–	–	–	–	–	–	–	–	–	–	–	–	74.0	7.147	–	–
6481.878	Fe I	2.28	−2.97	cn	78.4	7.401	–	–	–	–	–	–	–	–	–	–	59.1	7.119	–	–
6551.676	Fe I	0.99	−5.79	nd	–	–	–	–	–	–	–	–	58.2	7.187	–	–	–	–	–	–
6593.884	Fe I	2.43	−2.42	cn	97.7	7.381	–	–	–	–	–	–	–	–	–	–	–	–	–	–
6597.561	Fe I	4.80	−1.06	lz	40.4	7.379	–	–	57.0	7.171	58.7	7.155	60.3	7.276	51.2	7.118	29.6	7.210	66.1	7.401
6608.024	Fe I	2.28	−4.04	nd	20.6	7.306	92.2	7.638	–	–	–	–	–	–	–	–	–	–	–	–
6609.118	Fe I	2.56	−2.66	cn	71.3	7.233	–	–	–	–	–	–	–	–	–	–	–	–	–	–
6646.932	Fe I	2.61	−3.99	nd	14.0	7.397	–	–	–	–	–	–	48.4	7.302	50.3	7.288	–	–	–	–
6703.576	Fe I	2.76	−3.16	lz	42.5	7.400	–	–	–	–	74.5	6.942	95.8	7.433	92.6	7.340	–	–	–	–
6716.220	Fe I	4.58	−1.93	nd	16.9	7.467	–	–	–	–	–	–	–	–	–	–	–	–	–	–
6725.353	Fe I	4.19	−2.30	nd	15.0	7.378	55.9	7.741	42.2	7.367	26.8	7.039	37.0	7.362	–	–	–	–	–	–
6726.673	Fe I	4.61	−1.00	cn	43.8	7.186	81.7	7.441	62.6	6.958	–	–	70.5	7.155	59.0	6.954	35.8	7.084	69.9	7.170
6733.151	Fe I	4.64	−1.58	lz	18.4	7.222	64.8	7.745	52.1	7.395	32.7	6.991	–	–	52.5	7.455	–	–	52.7	7.473
6745.090	Fe I	4.58	−2.17	nd	–	–	40.4	7.812	–	–	19.9	7.211	22.8	7.398	–	–	–	–	–	–
6746.932	Fe I	2.61	−4.25	nd	–	–	–	–	–	–	–	–	23.0	7.079	–	–	–	–	–	–
6752.716	Fe I	4.64	−1.20	bk	29.1	7.121	–	–	–	–	–	–	–	–	84.0	7.625	–	–	–	–
6786.856	Fe I	4.19	−2.06	nd	26.6	7.459	71.6	7.779	47.6	7.221	–	–	55.3	7.438	46.7	7.281	–	–	–	–
6806.856	Fe I	2.73	−3.21	lz	43.0	7.421	–	–	–	–	80.9	7.054	92.6	7.379	89.8	7.294	25.7	7.161	99.7	7.515
6810.267	Fe I	4.61	−0.99	cn	51.5	7.311	91.6	7.605	76.5	7.177	–	–	77.0	7.249	67.1	7.077	34.5	7.040	79.2	7.320
6828.596	Fe I	4.64	−0.92	lz	59.0	7.412	–	–	97.6	7.503	73.2	7.065	91.4	7.468	93.8	7.510	45.2	7.207	–	–
6839.835	Fe I	2.56	−3.45	lz	42.9	7.477	–	–	–	–	76.6	6.997	97.6	7.483	–	–	–	–	–	–
6841.341	Fe I	4.61	−0.75	nd	–	–	–	–	–	–	–	–	–	–	–	–	61.6	7.301	–	–
6842.689	Fe I	4.64	−1.32	lz	–	–	85.0	7.853	70.0	7.438	55.7	7.151	67.4	7.453	67.6	7.455	–	–	69.1	7.507
6843.655	Fe I	4.55	−0.93	lz	62.3	7.390	–	–	97.5	7.394	–	–	–	–	88.0	7.305	49.8	7.211	–	–
6858.155	Fe I	4.61	−0.93	cn	59.7	7.403	97.6	7.656	83.6	7.238	–	–	81.5	7.268	85.5	7.336	–	–	86.1	7.387
6999.885	Fe I	4.10	−1.56	nd	–	–	–	–	91.9	7.331	–	–	90.7	7.418	–	–	–	–	96.1	7.549
7022.957	Fe I	4.19	−1.25	nd	–	–	–	–	87.6	7.066	92.7	7.171	–	–	98.7	7.344	–	–	–	–
7071.866	Fe I	4.61	−1.70	lz	–	–	68.8	7.891	51.7	7.463	42.2	7.246	–	–	–	–	–	–	55.9	7.605
7112.170	Fe I	2.99	−2.99	cn	–	–	–	–	–	–	–	–	88.5	7.400	98.3	7.532	–	–	–	–
7132.985	Fe I	4.07	−1.63	cn	47.5	7.308	93.8	7.573	75.3	7.077	–	–	69.6	7.079	77.6	7.199	35.5	7.142	77.6	7.234
7219.680	Fe I	4.07	−1.35	ow	–	–	–	–	–	–	93.6	7.119	–	–	–	–	–	–	–	–
7284.842	Fe I	4.14	−1.75	nd	–	–	80.1	7.528	–	–	70.8	7.193	–	–	–	–	–	–	–	–
7306.570	Fe I	4.18	−1.74	lz	–	–	99.5	7.909	65.8	7.168	–	–	77.9	7.454	68.5	7.285	–	–	72.9	7.388
7401.691	Fe I	4.19	−1.60	cn	46.4	7.366	91.9	7.638	75.3	7.189	64.9	6.994	76.1	7.289	73.2	7.229	32.9	7.168	92.7	7.604
7418.672	Fe I	4.14	−1.38	ow	–	–	–	–	80.7	6.987	–	–	83.4	7.126	80.3	7.061	38.4	7.001	87.6	7.226
7443.026	Fe I	4.19	−1.82	nd	–	–	85.5	7.742	–	–	–	–	–	–	–	–	25.8	7.232	–	–
7583.796	Fe I	3.02	−1.88	cn	89.2	7.197	–	–	–	–	–	–	–	–	–	–	–	–	–	–
7710.367	Fe I	4.22	−1.11	cn	–	–	–	–	99.0	7.107	93.1	7.023	–	–	–	–	54.1	7.086	–	–
7723.210	Fe I	2.28	−3.62	fm	39.9	7.234	–	–	–	–	–	–	98.3	7.206	–	–	–	–	–	–
7746.605	Fe I	5.06	−1.34	nd	–	–	58.1	7.874	–	–	–	–	34.0	7.355	42.8	7.519	–	–	–	–

Table 2 (continued)

λ (Å)	Ion	χ	log gf	Ref.	HD 4395		HD 180622		HD 201657		HD 201824		HD 210946		HD 211594		HD 216219		HD 223617	
					EW	log ϵ	EW	log ϵ	EW	log ϵ	EW	log ϵ	EW	log ϵ	EW	log ϵ	EW	log ϵ	EW	log ϵ
7751.116	Fe I	4.99	−0.72	cn	40.4	7.175	–	–	–	–	–	–	79.7	7.440	–	–	33.8	7.092	–	–
7780.568	Fe I	4.47	−0.09	cn	–	–	–	–	–	–	–	–	–	–	–	–	98.9	7.062	–	–
7941.096	Fe I	3.27	−2.58	nd	51.6	7.445	–	–	–	–	–	–	72.8	7.036	73.6	7.005	–	–	–	–
5991.378	Fe II	3.15	−3.56	cn	37.6	7.279	46.8	7.732	–	–	–	–	–	–	–	–	43.8	7.346	–	–
6084.110	Fe II	3.20	−3.97	nd	20.3	7.318	–	–	–	–	–	–	–	–	–	–	–	–	–	–
6149.249	Fe II	3.89	−2.72	cn	37.8	7.189	–	–	–	–	–	–	–	–	–	–	45.4	7.281	47.4	7.536
6247.562	Fe II	3.89	−2.26	lh	68.5	7.371	–	–	51.7	7.319	–	–	64.5	7.351	–	–	–	–	62.1	7.412
6369.462	Fe II	2.89	−4.36	nd	29.5	7.628	–	–	–	–	–	–	–	–	–	–	–	–	–	–
6416.928	Fe II	3.89	−2.74	cn	–	–	–	–	–	–	50.6	7.109	–	–	–	–	–	–	–	–
6432.683	Fe II	2.89	−3.58	cn	52.4	7.344	58.9	7.738	46.1	7.308	–	–	57.4	7.354	–	–	53.4	7.273	51.2	7.316
6456.391	Fe II	3.90	−2.07	cn	76.1	7.335	–	–	–	–	–	–	77.1	7.435	–	–	–	–	–	–
7711.731	Fe II	3.90	−2.47	cn	47.6	7.087	–	–	–	–	66.4	7.161	–	–	–	–	–	–	59.5	7.570
6154.230	Na I	2.10	−1.57	cn	28.7	6.007	125.2	6.688	86.4	5.993	53.0	5.829	–	–	83.3	6.145	24.7	5.987	96.6	6.369
6160.753	Na I	2.10	−1.23	cn	55.1	6.102	141.6	6.583	112.1	5.993	81.3	5.890	101.7	6.123	104.5	6.090	34.8	5.843	117.1	6.323
5528.418	Mg I	4.34	−0.78	nd	–	–	–	–	–	–	–	–	–	–	–	–	193.0	7.286	–	–
5711.095	Mg I	4.34	−1.82	nd	80.3	7.126	162.8	7.780	151.0	7.416	136.7	7.463	82.6	6.606	–	–	88.4	7.288	146.3	7.555
7657.606	Mg I	5.11	−1.19	nd	91.3	7.265	–	–	–	–	104.6	7.103	–	–	111.5	7.148	80.8	7.176	153.1	7.722
6696.020	Al I	3.14	−1.33	lw	43.3	6.211	–	–	–	–	–	–	–	–	–	–	–	–	–	–
6698.670	Al I	3.14	−1.87	cn	19.7	6.275	105.9	6.987	71.4	6.374	43.0	6.207	50.8	6.321	64.4	6.452	13.3	6.134	56.0	6.352
7835.317	Al I	4.02	−0.58	cn	42.5	6.258	129.3	7.032	110.5	6.653	67.6	6.304	–	–	–	–	23.3	5.944	–	–
7836.130	Al I	4.02	−0.40	cn	48.7	6.169	111.8	6.625	88.4	6.201	67.9	6.128	96.5	6.488	68.5	6.055	40.9	6.092	–	–
5665.563	Si I	4.92	−2.04	cn	37.0	7.382	103.6	–	–	–	–	–	–	–	–	–	32.8	7.330	78.9	7.918
5690.433	Si I	4.93	−1.87	cn	–	–	79.3	7.882	–	–	–	–	–	–	–	–	–	–	–	–
5701.108	Si I	4.93	−2.05	cn	51.6	7.655	–	–	67.1	7.749	–	–	57.0	7.524	43.9	7.329	31.7	7.328	66.7	7.729
5772.149	Si I	5.08	−1.67	cn	47.9	7.349	–	–	–	–	–	–	–	–	–	–	46.0	7.338	88.1	7.882
5793.079	Si I	4.93	−1.95	cn	53.7	7.582	88.1	8.112	76.9	7.810	–	–	62.1	7.505	71.7	7.701	43.7	7.438	71.4	7.706
5948.548	Si I	5.08	−1.19	cn	84.7	7.447	–	–	–	–	84.6	7.127	–	–	120.5	7.866	74.7	7.304	–	–
6125.026	Si I	5.61	−1.54	lz	42.5	7.642	–	–	–	–	–	–	–	–	77.7	8.177	–	–	–	–
6142.494	Si I	5.62	−1.48	ns	–	–	58.0	7.940	–	–	–	–	–	–	–	–	31.8	7.415	50.8	7.686
6145.020	Si I	5.62	−1.43	ns	41.2	7.519	–	–	55.3	7.771	41.3	7.253	–	–	29.7	7.229	32.1	7.370	53.5	7.685
7034.910	Si I	5.87	−0.81	cn	51.7	7.279	83.7	8.001	–	–	53.7	7.135	–	–	60.1	7.463	51.9	7.287	–	–
7226.208	Si I	5.61	−1.30	nd	35.1	7.226	–	–	–	–	49.5	7.235	61.4	7.617	–	–	32.4	7.189	68.9	7.801
7405.790	Si I	5.61	−0.68	cn	84.2	7.360	118.4	8.070	110.9	7.855	97.6	7.404	–	–	119.4	7.884	82.5	7.334	115.6	7.889
7415.958	Si I	5.61	−0.71	cn	94.9	7.549	–	–	–	–	–	–	–	–	–	–	93.4	7.524	–	–
7918.383	Si I	5.95	−0.54	cn	79.9	7.433	–	–	–	–	–	–	–	–	–	–	65.8	7.245	–	–
7932.351	Si I	5.96	−0.35	cn	106.1	7.576	98.0	7.823	–	–	134.4	7.982	83.7	7.411	93.4	7.574	94.9	7.435	–	–
5512.989	Ca I	2.93	−0.53	cn	–	–	–	–	132.5	5.968	135.4	6.507	107.3	5.885	136.1	6.242	80.8	6.172	–	–
5581.979	Ca I	2.52	−0.67	cn	111.3	6.364	–	–	192.2	6.336	153.5	6.440	147.9	6.179	184.3	6.481	98.7	6.222	159.5	6.358
5588.764	Ca I	2.52	0.06	cn	–	–	–	–	191.1	5.592	197.6	6.219	183.7	5.855	186.5	5.769	–	–	190.1	5.953
5590.126	Ca I	2.52	−0.70	cn	102.6	6.267	–	–	–	–	118.7	5.864	128.0	5.908	133.2	5.890	93.1	6.164	149.8	6.255
5601.286	Ca I	2.52	−0.52	cn	125.8	6.411	–	–	162.9	5.867	120.8	5.724	–	–	161.5	6.095	106.7	6.191	–	–
5867.572	Ca I	2.93	−1.61	cn	–	–	81.9	6.367	–	–	–	–	45.4	5.942	43.3	5.830	18.5	6.101	–	–
6102.727	Ca I	1.88	−0.79	nd	138.6	6.156	–	–	–	–	189.2	6.077	191.3	5.886	–	–	–	–	–	–
6122.226	Ca I	1.89	−0.32	nd	185.2	6.107	–	–	–	–	199.5	5.727	–	–	–	–	–	–	–	–
6161.295	Ca I	2.52	−1.19	cn	75.0	6.264	–	–	–	–	129.5	6.452	112.4	6.060	128.6	6.221	54.4	5.981	–	–
6163.754	Ca I	2.52	−1.07	nd	–	–	–	–	–	–	136.0	6.429	–	–	–	–	–	–	–	–
6166.440	Ca I	2.52	−1.19	cn	68.2	6.144	130.4	6.214	133.1	6.009	103.8	5.987	110.8	6.030	121.9	6.112	57.3	6.030	117.3	6.116
6169.044	Ca I	2.52	−0.80	lz	97.9	6.251	–	–	–	–	125.2	5.980	145.3	6.168	125.2	5.773	82.0	6.048	153.7	6.293
6169.564	Ca I	2.52	−0.51	cn	–	–	–	–	–	–	128.4	5.750	163.3	6.115	150.8	5.853	99.5	6.048	158.5	6.071
6439.083	Ca I	2.52	0.16	cn	168.9	6.201	–	–	185.7	5.328	166.5	5.625	193.5	5.763	188.4	5.604	148.9	5.998	–	–
6449.820	Ca I	2.52	−0.50	cn	122.2	6.316	–	–	–	–	–	–	–	–	157.7	5.915	–	–	–	–
6455.605	Ca I	2.52	−1.29	cn	–	–	–	–	110.9	5.736	–	–	93.3	5.821	100.7	5.847	–	–	105.4	5.981
6471.668	Ca I	2.52	−0.69	cn	94.9	6.159	–	–	–	–	123.5	5.822	139.9	6.006	–	–	83.7	6.009	–	–
6493.788	Ca I	2.52	−0.09	cn	–	–	–	–	–	–	168.1	5.952	178.6	5.954	185.6	5.942	116.9	5.981	–	–

Table 2 (continued)

λ (Å)	Ion	χ	log gf	Ref.	HD 4395		HD 180622		HD 201657		HD 201824		HD 210946		HD 211594		HD 216219		HD 223617	
					EW	log ϵ	EW	log ϵ	EW	log ϵ	EW	log ϵ	EW	log ϵ	EW	log ϵ	EW	log ϵ	EW	log ϵ
6499.654	Ca I	2.52	−0.81	cn	88.6	6.156	–	–	141.4	5.750	106.0	5.620	127.5	5.921	129.3	5.856	71.0	5.893	139.2	6.096
6717.687	Ca I	2.71	−0.52	cn	–	–	–	–	196.9	6.333	156.8	6.364	–	–	179.2	6.393	107.0	6.322	–	–
7148.150	Ca I	2.71	−0.14	cn	–	–	–	–	–	–	–	–	191.7	6.180	190.5	6.058	137.2	6.292	189.5	6.179
5526.821	Sc II	1.77	0.13	nd	–	–	122.6	3.138	124.5	2.867	146.1	3.158	124.8	3.011	142.4	3.307	96.5	2.936	124.3	3.072
5657.880	Sc II	1.51	−0.50	nd	81.5	3.056	121.3	3.384	102.2	2.734	104.2	2.617	96.0	2.766	102.4	2.887	85.1	3.069	110.2	3.080
5684.198	Sc II	1.51	−0.20	nd	–	–	–	–	–	–	–	–	–	–	110.0	2.725	79.8	2.668	–	–
6245.620	Sc II	1.51	−0.98	lz	–	–	–	–	–	–	97.2	2.894	–	–	98.0	3.233	–	–	–	–
6604.600	Sc II	1.36	−1.16	lz	51.3	2.926	114.9	3.585	102.3	3.101	–	–	86.2	2.990	90.8	3.068	51.1	2.887	–	–
5866.461	Ti I	1.07	−0.84	cn	42.2	4.519	178.3	5.360	141.3	4.315	86.0	3.949	117.1	4.444	110.6	4.196	36.0	4.522	–	–
5953.170	Ti I	1.89	−0.21	cn	50.6	4.899	140.0	5.158	100.3	4.140	83.5	4.353	–	–	–	–	25.8	4.515	104.1	4.623
6126.224	Ti I	1.07	−1.32	cn	29.3	4.731	129.7	4.875	131.7	4.556	108.9	4.760	93.7	4.494	114.3	4.689	–	–	112.8	4.736
6258.110	Ti I	1.44	−0.43	cn	57.8	4.757	–	–	–	–	109.7	4.381	–	–	–	–	40.2	4.557	135.0	4.743
6261.106	Ti I	1.43	−0.48	cn	65.1	4.925	–	–	137.8	4.313	109.2	4.406	121.3	4.577	–	–	–	–	–	–
6312.241	Ti I	1.46	−1.55	lz	–	–	75.4	4.693	52.0	4.147	32.2	4.280	40.0	4.432	–	–	–	–	57.5	4.597
6599.110	Ti I	0.90	−2.08	lz	–	–	–	–	73.4	4.146	39.6	4.178	62.5	4.529	–	–	–	–	84.9	4.736
6743.120	Ti I	0.90	−1.63	lz	12.1	4.332	133.9	4.857	–	–	55.9	3.952	84.1	4.349	–	–	–	–	107.6	4.603
5727.057	V I	1.08	−0.01	cn	–	–	164.1	4.431	–	–	–	–	128.3	3.907	194.5	4.807	41.1	3.806	–	–
6090.216	V I	1.08	−0.14	cn	36.7	3.710	138.6	3.948	109.7	3.081	–	–	91.6	3.326	81.6	3.036	18.3	3.410	113.8	3.631
6216.358	V I	0.28	−0.75	lz	–	–	162.5	3.772	–	–	–	–	103.2	2.940	70.3	2.349	–	–	137.5	3.440
5783.866	Cr I	3.32	−0.20	cn	45.4	5.478	116.7	5.902	111.7	5.570	–	–	86.9	5.451	106.3	5.713	32.6	5.299	108.1	5.826
5787.926	Cr I	3.32	−0.18	cn	38.5	5.333	109.6	5.749	86.3	5.118	75.2	5.263	70.7	5.158	62.1	4.939	31.7	5.266	87.8	5.430
6925.280	Cr I	3.45	−0.33	nd	40.2	5.587	–	–	61.7	4.979	60.9	5.246	62.9	5.269	45.9	4.930	24.3	5.322	–	–
6978.383	Cr I	3.46	0.14	cn	63.1	5.536	–	–	–	–	–	–	–	–	–	–	–	–	–	–
6979.806	Cr I	3.46	−0.41	lz	30.6	5.484	106.3	5.952	–	–	73.1	5.538	80.5	5.637	85.4	5.655	22.7	5.371	97.1	5.886
7355.891	Cr I	2.89	−0.29	cn	63.0	5.351	155.6	5.806	–	–	89.9	4.927	–	–	–	–	54.4	5.272	152.4	5.860
7400.188	Cr I	2.90	−0.17	cn	67.2	5.315	164.7	5.825	137.9	5.168	–	–	126.4	5.369	120.9	5.191	–	–	140.6	5.571
6013.497	Mn I	3.07	−0.15	lz	94.8	5.413	177.0	5.800	140.0	5.004	124.5	5.102	138.4	5.270	136.7	5.164	67.2	4.989	147.9	5.449
6021.803	Mn I	3.07	0.02	lz	68.5	4.778	170.2	5.555	138.4	4.810	121.0	4.864	137.7	5.090	132.5	4.933	64.5	4.773	147.3	5.271
5578.729	Ni I	1.68	−2.80	cn	–	–	–	–	–	–	135.5	6.412	–	–	146.8	6.608	–	–	124.7	6.324
5587.868	Ni I	1.93	−2.14	fm	–	–	–	–	–	–	128.4	5.930	137.3	6.167	–	–	62.5	5.750	–	–
5593.746	Ni I	3.90	−0.84	cn	51.9	6.202	93.2	6.575	77.1	6.079	66.4	5.835	67.7	5.988	82.9	6.254	38.0	5.990	–	–
5625.328	Ni I	4.09	−0.70	fm	–	–	–	–	–	–	–	–	–	–	86.5	6.400	39.1	6.056	–	–
5694.991	Ni I	4.09	−0.61	cn	48.4	6.091	–	–	85.1	6.222	64.9	5.802	73.7	6.085	71.5	6.046	40.6	5.991	–	–
5754.666	Ni I	1.93	−2.33	fm	–	–	–	–	–	–	138.3	6.278	–	–	130.0	6.142	69.5	6.056	–	–
5805.226	Ni I	4.17	−0.64	cn	–	–	72.2	6.297	49.7	5.742	–	–	63.9	6.033	–	–	–	–	–	–
6086.288	Ni I	4.26	−0.53	cn	44.3	6.088	–	–	62.5	5.961	73.0	6.060	60.6	5.963	–	–	29.8	5.850	67.2	6.116
6108.125	Ni I	1.68	−2.63	lz	72.1	6.033	149.6	6.512	147.3	6.103	–	–	132.2	6.138	–	–	53.9	5.776	134.2	6.222
6111.078	Ni I	4.09	−0.81	fm	30.6	5.927	76.5	6.436	–	–	–	–	62.9	6.076	–	–	–	–	74.3	6.316
6128.984	Ni I	1.68	−3.33	fm	36.7	6.074	117.8	6.636	89.0	5.812	80.1	5.718	80.2	5.903	71.9	5.725	16.8	5.699	92.7	6.129
6130.141	Ni I	4.26	−0.96	cn	25.6	6.139	63.3	6.555	–	–	43.9	5.951	38.8	6.004	–	–	14.4	5.872	40.3	6.047
6176.816	Ni I	4.09	−0.26	cn	–	–	–	–	–	–	–	–	97.0	6.117	–	–	52.9	5.842	99.6	6.228
6327.604	Ni I	1.68	−3.11	cn	40.5	5.911	132.5	6.654	120.0	6.098	94.6	5.737	94.9	5.915	84.6	5.699	25.2	5.686	108.7	6.184
6482.809	Ni I	1.93	−2.63	fm	46.0	5.785	132.6	6.477	110.8	5.785	–	–	–	–	–	–	–	–	–	–
6586.319	Ni I	1.95	−2.73	cn	55.4	6.071	120.0	6.359	90.3	5.560	–	–	105.3	6.039	–	–	27.4	5.624	106.4	6.082
6635.150	Ni I	4.42	−0.83	lz	25.7	6.143	86.2	7.014	–	–	52.0	6.140	–	–	–	–	20.9	6.067	–	–
6643.638	Ni I	1.68	−2.30	fm	107.5	6.300	–	–	168.1	5.964	133.0	5.601	160.3	6.131	–	–	87.4	6.007	177.0	6.410
6767.784	Ni I	1.83	−2.17	cn	82.3	5.859	171.6	6.421	141.4	5.638	–	–	–	–	–	–	71.4	5.732	148.8	6.061
6772.321	Ni I	3.66	−0.95	lz	48.2	5.938	–	–	87.6	6.009	63.9	5.528	83.2	6.014	78.6	5.937	35.5	5.753	89.7	6.171
7001.600	Ni I	1.94	−3.66	nd	13.4	6.031	85.6	6.611	–	–	38.7	5.619	48.0	5.981	43.5	5.872	–	–	–	–
7030.010	Ni I	3.54	−1.73	nd	20.2	5.995	–	–	–	–	30.4	5.542	39.4	5.893	–	–	14.9	5.891	–	–
7110.905	Ni I	1.93	−2.92	nd	46.5	6.036	147.6	6.889	142.2	6.480	–	–	–	–	125.7	6.428	20.6	5.589	–	–
7122.206	Ni I	3.54	0.04	cn	–	–	–	–	–	–	162.5	6.031	–	–	–	–	98.6	5.691	194.5	6.417
7385.244	Ni I	2.74	−1.97	cn	57.7	6.128	145.6	6.934	108.7	6.095	74.0	5.509	83.5	5.840	99.2	6.078	28.1	5.646	97.5	6.100
7414.514	Ni I	1.99	−2.57	cn	–	–	–	–	–	–	120.3	5.923	–	–	–	–	61.4	6.073	–	–

Table 2 (continued)

λ (Å)	Ion	χ	log gf	Ref.	HD 4395		HD 180622		HD 201657		HD 201824		HD 210946		HD 211594		HD 216219		HD 223617	
					EW	log ϵ	EW	log ϵ	EW	log ϵ	EW	log ϵ	EW	log ϵ	EW	log ϵ	EW	log ϵ	EW	log ϵ
7422.286	Ni I	3.63	−0.33	cn	88.9	5.939	180.4	6.816	154.5	6.266	135.2	6.066	–	–	151.4	6.301	82.4	5.865	–	–
7525.118	Ni I	3.63	−0.65	cn	78.8	6.092	152.3	6.823	131.4	6.284	120.8	6.143	–	–	128.6	6.323	59.0	5.796	–	–
7574.048	Ni I	3.83	−0.61	cn	63.5	5.986	116.3	6.499	93.9	5.937	84.6	5.709	101.9	6.128	93.0	5.983	51.2	5.818	106.2	6.257
7714.310	Ni I	1.93	−1.91	cn	110.0	6.085	–	–	–	–	178.1	6.094	–	–	195.7	6.251	87.6	5.779	–	–
7715.591	Ni I	3.70	−0.95	cn	43.0	5.832	123.8	6.792	68.3	5.701	66.0	5.567	93.1	6.164	68.9	5.770	33.5	5.704	92.1	6.208
7727.616	Ni I	3.68	−0.17	cn	–	–	154.5	6.421	–	–	–	–	130.3	5.930	113.4	5.664	77.9	5.663	–	–
7748.894	Ni I	3.70	−0.33	cn	82.6	5.883	141.1	6.445	121.5	5.891	108.4	5.683	128.6	6.086	101.2	5.657	74.7	5.788	124.7	6.121
7788.933	Ni I	1.95	−2.42	fm	–	–	196.8	7.008	155.9	6.114	125.4	5.762	–	–	137.1	6.038	75.3	6.089	–	–
7797.588	Ni I	3.90	−0.30	lz	78.0	5.975	–	–	90.8	5.656	92.3	5.599	–	–	91.5	5.722	60.6	5.724	–	–
6435.000	Y I	0.07	−0.82	hl	10.4	2.560	126.9	2.896	132.1	2.552	96.0	2.300	83.3	2.354	126.0	2.871	–	–	108.2	2.642
6127.460	Zr I	0.15	−1.06	bg	6.5	2.833	119.6	3.231	110.8	2.677	–	–	–	–	87.1	2.769	7.5	3.042	80.0	3.181
6134.570	Zr I	0.00	−1.28	bg	4.4	2.711	111.7	3.031	106.9	2.568	76.6	2.480	82.3	2.776	–	–	5.9	2.997	71.6	2.976
6140.460	Zr I	0.52	−1.41	bg	–	–	76.8	3.444	88.4	3.307	–	–	58.3	3.435	–	–	–	–	–	–
6143.180	Zr I	0.07	−1.10	bg	12.5	3.097	125.3	3.231	151.5	3.279	117.6	3.127	100.9	2.980	132.5	3.396	15.6	3.360	92.2	3.292
5853.688	Ba II	0.60	−1.01	wm	112.5	2.559	171.7	2.888	257.0	3.110	268.5	3.215	182.6	2.790	252.5	3.214	160.0	3.039	197.1	3.010
6141.727	Ba II	0.70	−0.08	wm	186.9	2.423	249.9	2.619	477.9	2.972	416.2	2.863	303.2	2.639	485.0	3.094	258.2	2.745	311.0	2.755
6496.908	Ba II	0.60	−0.38	wm	178.7	2.517	270.8	2.854	431.1	3.013	378.4	2.921	288.9	2.725	445.7	3.164	222.3	2.735	302.8	2.871
6390.480	La II	0.32	−1.45	lb	–	–	73.5	1.999	108.6	2.292	95.0	2.040	68.2	1.859	88.1	2.185	32.9	1.933	81.4	2.109
6645.110	Eu II	1.37	0.20	bc	19.1	0.776	59.6	1.236	50.3	0.829	58.8	0.774	27.2	0.500	45.6	0.880	16.1	0.656	48.2	0.938

bc: Biémont et al. (1982); bg: Biémont et al. (1981); bk: Bard & Kock (1994); cn: Chen et al. (2000b); fm: Fuhr et al. (1988); hl: Hannaford et al. (1982); lb: Luck & Bond (1991); lh: Lambert et al. (1996); lw: Lambert & Warner (1968); lz: Liang et al. (2003); nd: NIST database (*http://physics.nist.gov*); ns: Nissen & Schuster (1997); ow: O'Brian et al. (1991); wm: Weise & Martin (1980).

3 STELLAR ATMOSPHERIC PARAMETERS

The stellar atmospheric model is composed of four basic parameters, i.e., effective temperature, surface gravity, metallicity and microturbulent velocity. In this section, we describe the determinations of these four model-atmosphere parameters. The abundance patterns of the sample stars will be given in Section 5 (see Fig. 3).

3.1 Effective Temperature

Effective temperatures $T_{\rm eff}$ were determined from [Fe/H] and $B-V$ color indices by using the empirical calibration of Alonso et al. (1999, 2001), which is suitable for giant stars. We use $B-V$ color here since the $B-V$ data are more complete than other color indices for the sample stars. Considering the uncertainties in photometric data, [Fe/H], and the errors in the calibration relation, we estimate the uncertainty in $T_{\rm eff}$ is about 100 K for our sample stars.

3.2 Surface Gravity

Based on the *Hipparcos* parallaxes, precise values of the surface gravity of nearby stars can be obtained using the following relations:

$$\log\frac{g}{g_\odot} \;=\; \log\frac{\mathcal{M}}{\mathcal{M}_\odot} + 4\log\frac{T_{\rm eff}}{T_{\rm eff\,\odot}} + 0.4\,(M_{\rm bol} - M_{\rm bol,\odot}) \qquad (2)$$

and

$$M_{\rm bol} \;=\; V + BC + 5\log\pi + 5, \qquad (3)$$

where $\mathcal{M}$ is the stellar mass, $M_{\rm bol}$ the absolute bolometric magnitude, V the visual magnitude, BC the bolometric correction, and π the parallax. We adopt the solar values $\log g_\odot = 4.44$, $T_{\rm eff,\odot} = 5770$ K,

$M_{\rm bol,\odot} = 4.77$ mag. The parallax π and its errors are taken from the Hipparcos Satellite observations (ESA 1997). Stellar mass was determined from the position of the star in the $M_{\rm bol} - \log T_{\rm eff}$ diagram. We adopt the stellar evolutionary tracks of Yonsei-Yale (Yi et al. 2003), whose isochrones, which were determined with high quality observational data, cover the stage from pre-main-sequence birthline to the helium-core flash. The uncertainty of $\log g$ estimated by this method is generally about 0.2 dex for our sample stars.

3.3 Metal Abundance

The initial metallicities of the sample stars in their model atmospheres were taken from literature if available. Otherwise, we adopt [Fe/H]=0 as the initial value and then the final model metallicitiy was derived from the consistency with the other parameters in the abundance calculation. The estimated error in [Fe/H] is about 0.1 dex.

3.4 Microturbulence Velocity

The value of microturbulence velocity ξ_t was determined from the abundance analysis by requiring a null correlation between [Fe/H] and the EWs. We applied this calculation with a large range of EWs ($20-150$ mÅ) for Fe I lines. With this selection, the uncertainty in the microturbulence velocity is about 0.2 km s^{-1}.

Table 3 presents the atmospheric parameters for the sample stars, where columns (1)–(6) list the HD identifications, $T_{\rm eff}$, $\log g$, mass, microturbulence velocity and [Fe/H]. The temperature coverage of the stars is from 4284 to 5553 K; the surface gravity coverage is from 1.67 to 3.64. The microturbulence velocity is from 1.3 to 1.7 and their [Fe/H] is from -0.40 to 0.21. The uncertainties of the parameters are: $\sigma(T_{\rm eff}) = 100$ K, $\sigma(\log g) = 0.2$, $\sigma([{\rm Fe/H}]) = 0.1$ and $\sigma(\xi_t) = 0.2$ km s^{-1}.

Table 3 Atmospheric Parameters of the Sample Stars

HD	$T_{\rm eff}$	$\log g$	$M/M_\odot$	ξ_t	[Fe/H]
4395	5447	3.60	1.60(+0.13,−0.10)	1.3	−0.16
180622	4391	2.24	1.92(+1.07,−0.36)	1.5	0.21
201657	4284	2.17	0.78(+0.08,−0.02)	1.7	−0.31
201824	4552	1.67	4.58(−,−3.32)	1.5	−0.40
210946	4577	2.42	1.40(+0.72,−0.28)	1.6	−0.22
211594	4490	2.44	0.90(+0.41,−0.09)	1.6	−0.23
216219	5553	3.64	1.48(+0.07,−0.08)	1.4	−0.34
223617	4501	2.27	1.78(+0.47,−0.33)	1.5	−0.10

The reliability of the derived atmospheric parameters $T_{\rm eff}$/$\log g$/ξ_t have been confirmed by further checks. Taking HD 216219 as a representative, Figure 4a gives the Fe abundances from different Fe I lines as a function of their excitation potential, which fulfills the excitation equilibrium; Figure 4b shows that the Fe abundances from Fe I lines and Fe II lines are consistent within 0.2 dex, which illustrates the ionization equilibrium and also shows that there is no trend between Fe abundances and the EWs of the lines.

Comparing our results with those of Smith et al. (1993), the derived atmospheric parameters for HD 4395 are $T_{\rm eff}$=5447/5450 K, $\log g = 3.60/3.3$, $\xi_t = 1.3/1.3$, [Fe/H]$= -0.16/-0.33$; for HD 216219 are $T_{\rm eff} = 5553/5600$ K, $\log g = 3.64/3.2$, $\xi_t = 1.4/1.6$, [Fe/H]$= -0.34/-0.32$. They are very consistent.

4 STELLAR ATMOSPHERIC MODEL AND SPECTRAL LINES

The stellar atmospheric model is implemented by the ATLAS9 code (Kurucz 1993) to do the abundance analysis. This uses LTE, plane-parallel and line-blanketed models. Abundances of chemical elements

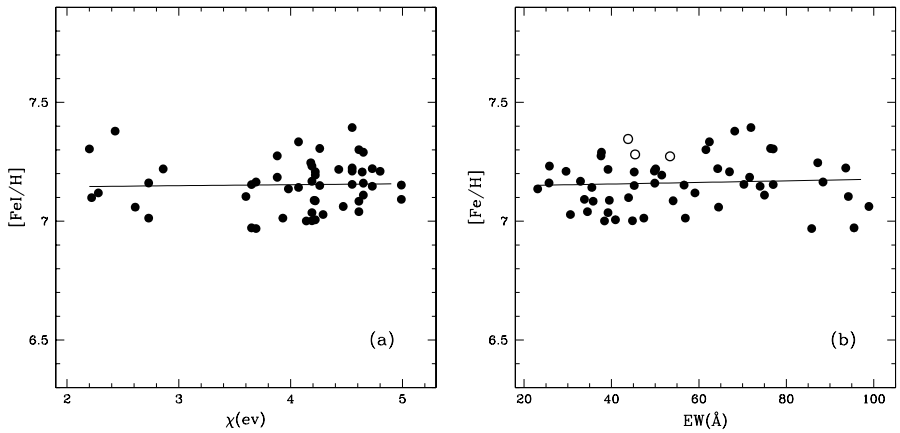

Fig. 4 To check the reliability of the determined atmospheric parameters $T_{\rm eff}/\log g/\xi_t$ of the stars by taking HD216219 as an example: (a) Fe abundances from Fe I lines as a function of excitation potential. There is no significant trend of [Fe/H] with χ, indicating a correct temperature distribution in the model atmosphere. (b) The consistency of the Fe I and Fe II abundances (the filled and open circles refer to the Fe I and Fe II abundances respectively), which means that the determined $\log g$ are reliable; and an illustration of the determination of the microturbulence velocity, since there is no significant trend between [Fe/H] and EWs.

were determined by using the input atmospheric parameters given in Table 3 and the measured EWs of the absorption lines. All the lines adopted in determining element abundances are presented in Table 2, which shows the spectral lines and wavelengths, excitation potential χ, oscillator strengths $\log gf$, EWs and $\log\epsilon$ of each line. The selections of the lines have been described in Section 2. The oscillator strengths $\log gf$ of spectral lines are taken from the NIST database (*http://physics.nist.gov*), Lambert & Warner (1968), Weise & Martin (1980), Biémont et al. (1981, 1982), Hannaford et al. (1982), Fuhr et al. (1988), Luck & Bond (1991), O'Brian et al. (1991), Bard & Kock (1994), Lambert et al. (1996), Nissen & Schuster (1997), Chen et al. (2000), Liang et al. (2003) and the references therein. Col. (5) of Table 2 gives these reference sources for the spectral lines.

5 CHEMICAL ABUNDANCES AND ANALYSIS

In this section, we present the determined abundances of the sample stars for about 20 elements based on the spectral observations and atmospheric model.

5.1 Abundance of Barium Stars

The derived element abundances of all the sample stars are given in Table 4, including $\log\epsilon$ and the corresponding [X/Fe] values for all ions. The solar abundances are adopted from Grevesse & Sauval (1998).

Figure 3 directly presents the abundance results of our sample stars, including the chemical elements, Na, Mg, Al, Si, Ca, Sc, Ti, V, Cr, Mn, Ni, Y, Zr, Ba, La and Eu. It obviously shows that the neutron capture process elements, Y, Zr, Ba, La and Eu, are more abundant than the solar values. In particular, Y and Zr exhibit the first peak while Ba and La exhibit the second peak, and the second peak is higher than the first one. Other elements from Na to Ni, such as α elements and iron elements, show similar abundances to the solar values, which means that these Ba stars belong to disk stars. The behavior of Sc and Mn is compatible with the results of Nissen et al. (2000) and Chen et al. (2000a), who demonstrated that [Sc/Fe] decreases with increasing metallicity in disk stars, whereas [Mn/Fe] increases with increasing [Fe/H].

Table 4 Element Abundances of the Sample Stars

	HD 4395			HD 180622			HD 201657			HD 201824		
[Fe/H]		–0.16			0.21			–0.31			–0.40	
Ion	N	log ϵ(X)	[X/Fe]	N	log ϵ(X)	[X/Fe]	N	log ϵ(X)	[X/Fe]	N	log ϵ(X)	[X/Fe]
Fe I	51	7.34	–	35	7.71	–	45	7.18	–	28	7.10	–
Fe II	8	7.32	–	2	7.73	–	2	7.31	–	2	7.14	–
Na I	2	6.05	−0.12	2	6.64	0.10	2	5.99	−0.03	2	5.86	−0.07
Mg I	2	7.20	−0.22	1	7.78	−0.01	1	7.42	0.15	2	7.28	0.10
Al I	4	6.23	−0.08	3	6.88	0.20	3	6.41	0.25	3	6.21	0.14
Si I	13	7.46	0.07	6	7.97	0.21	4	7.80	0.56	6	7.36	0.21
Ca I	12	6.23	0.03	2	6.29	−0.28	9	5.88	−0.17	17	6.03	0.07
Sc II	2	2.99	−0.02	3	3.37	−0.01	3	2.90	0.04	3	2.89	0.12
Ti I	6	4.69	−0.17	6	4.98	−0.25	6	4.27	−0.44	9	4.24	−0.38
V I	1	3.71	−0.13	3	4.05	−0.16	1	3.08	−0.61	0	–	–
Cr I	7	5.44	−0.07	5	5.85	−0.03	4	5.21	−0.15	4	5.24	−0.03
Mn I	2	5.10	−0.13	2	5.68	0.08	2	4.91	−0.17	2	4.98	−0.01
Ni I	25	6.02	−0.07	21	6.63	0.17	21	5.97	0.06	25	5.85	0.00
Y I	1	2.56	0.48	1	2.90	0.45	1	2.55	0.62	1	2.30	0.46
Zr I	3	2.88	0.44	4	3.23	0.42	3	2.84	0.67	2	2.80	0.60
Ba II	3	2.50	0.53	3	2.79	0.45	3	3.03	1.21	3	3.00	1.27
La II	0	–	–	1	2.00	0.62	1	2.29	1.43	1	2.04	1.27
Eu II	1	0.78	0.43	1	1.24	0.52	1	0.83	0.63	1	0.77	0.66
	HD 210946			HD 211594			HD 216219			HD 223617		
[Fe/H]		–0.22			–0.23			–0.34			–0.10	
Ion	N	log ϵ(X)	[X/Fe]	N	log ϵ(X)	[X/Fe]	N	log ϵ(X)	[X/Fe]	N	log ϵ(X)	[X/Fe]
Fe I	51	7.28	–	49	7.27	–	51	7.15	–	34	7.39	–
Fe II	3	7.38	–	0	–	–	3	7.30	–	4	7.46	–
Na I	1	6.12	0.01	2	6.12	0.02	2	5.91	−0.08	2	6.35	0.12
Mg I	2	6.98	−0.38	1	7.15	−0.2	3	7.25	0.01	2	7.64	0.16
Al I	2	6.40	0.15	2	6.25	0.01	3	6.06	−0.07	1	6.35	−0.02
Si I	4	7.51	0.18	8	7.65	0.33	13	7.35	0.14	8	7.79	0.34
Ca I	16	5.98	−0.16	18	6.03	−0.10	15	6.10	0.08	9	6.14	−0.12
Sc II	3	2.92	−0.03	5	3.04	0.10	4	2.89	0.06	3	3.11	0.04
Ti I	6	4.47	−0.33	2	4.44	−0.35	3	4.53	−0.15	6	4.67	−0.25
V I	3	3.39	−0.39	1	3.40	−0.37	2	3.61	−0.05	2	3.54	−0.36
Cr I	5	5.38	−0.07	5	5.29	−0.15	5	5.31	−0.02	5	5.71	0.14
Mn I	2	5.18	0.01	2	5.05	−0.11	2	4.88	−0.17	2	5.36	0.07
Ni I	21	6.03	0.00	20	6.04	0.02	30	5.83	−0.08	17	6.20	0.05
Y I	1	2.35	0.33	1	2.87	0.86	0	–	–	1	2.64	0.50
Zr I	3	3.06	0.68	2	3.08	0.71	3	3.13	0.87	3	3.15	0.65
Ba II	3	2.72	0.81	3	3.16	1.26	3	2.84	1.05	3	2.88	0.85
La II	1	1.86	0.91	1	2.18	1.24	1	1.93	1.10	1	2.11	1.04
Eu II	1	0.50	0.21	1	0.88	0.60	1	0.66	0.49	1	0.94	0.53

5.2 Uncertainties in the Abundances

There are two kinds of uncertainties in the abundance determination: the systematic errors introduced by the atmospheric parameters and the random errors in determining EWs, oscillator strengths and damping constants. We ignore the uncertainties in atomic data since they could be small (Chen et al. 2000b) and consider the uncertainties in atmospheric parameter determinations and EW measurements. Assuming that the effects of the uncertainties in the parameters are independent, we can estimate the total uncertainty with Equation (4):

$$\sigma_{\rm total} = \sqrt{(\sigma_{\rm EW})^2 + (\Delta T_{\rm eff})^2 + (\Delta \log g)^2 + (\Delta[{\rm Fe/H}])^2 + (\Delta \xi_t)^2}\,, \quad (4)$$

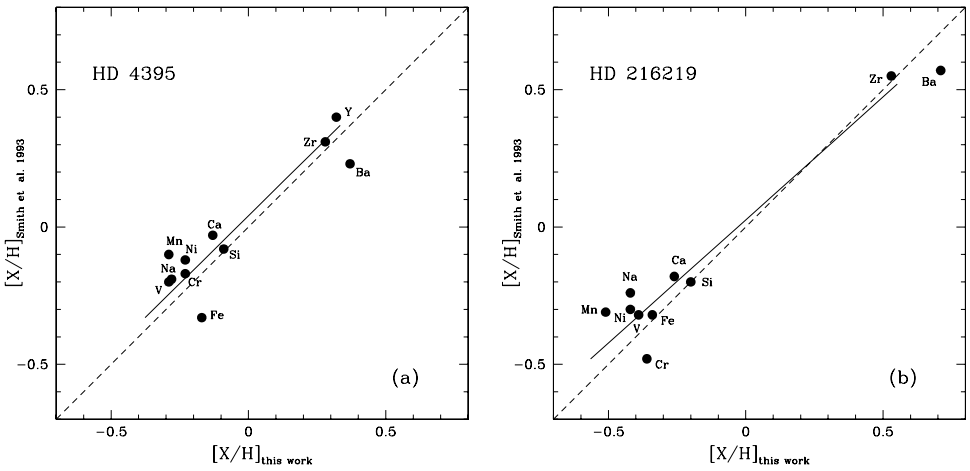

Fig. 5 Comparisons between our abundance determinations and those of Smith et al. (1993) for the two common stars: (a) for HD 4395; (b) for HD 216219. The solid lines are the least square fits for the data and the dashed lines are the one-to-one relations. Our results are consistent with theirs.

where $\sigma_{\rm EW}$, $\Delta T_{\rm eff}$, $\Delta \log g$, Δ[Fe/H] and $\Delta \xi_t$ are the corresponding variations in the ion abundances due to the variations in equivalent widths, $T_{\rm eff}$, $\log g$, metal abundance and microturbulent velocity, respectively.

For our spectra, the typical uncertainty of the EW is about 6.1%. Table 5 shows the effects on the derived abundances changed by 6.1% in EW, 100 K in effective temperature, 0.2 dex in surface gravity, 0.1 dex in metallicity and 0.2 km s^{-1} in microturbulence velocity for one representative star, HD 216219. The total uncertainties of the output abundances have also be given in Table 5 for all other sample stars by considering the same errors as above in the individual atmospheric parameters.

5.3 Comparisons with Smith et al. (1993)

As for the two stars also studied by Smith et al. (1993), we compare our abundance determinations with theirs for HD 4395 and HD 216219. Figure 5 shows the consistencies between our abundance estimations and theirs are within 0.2 dex, but most are within 0.1 dex.

6 COMPARING WITH WIND ACCRETION MODEL RESULTS

We try to use the wind accretion model to predict the theoretical heavy element abundances of Ba stars in binary systems, and then compare these theoretical predictions with the observed abundance patterns of our sample stars. Following Liang et al. (2000, 2003), the calculations of theoretical abundances are made in two steps: the AGB nucleosynthesis based on the latest TP-AGB model and the branch path of the s-process nucleosynthesis, and the binary accretion based on the angular momentum conservation model of wind accretion.

The standard case of our wind accretion model is: $M_{1,0} = 3.0\,M_{\odot}$, $M_{2,0} = 1.3\,M_{\odot}$, $v_{\rm ej} = 15\,{\rm km\,s^{-1}}$ ($M_{1,0}$ is the main sequence mass of the intrinsic AGB star, the current white dwarf, in the binary system; $M_{2,0}$ is the corresponding mass of the current Ba star; $v_{\rm ej}$ is the wind velocity). We assumed the standard accretion rate is 0.15 times that of Bondi-Hoyle's accretion rate (Liang et al. 2000; Boffin & Začs 1994). The observed orbital elements of the sample stars are listed in Table 6, which are taken from Jorissen et al. (1998) and Preston & Sneden (2001). The observed orbital periods of our sample stars cover 1018.9 to 6200 d and the eccentricities range from 0.06 to 0.65.

Figure 6 shows the comparisons between the theoretical abundances from the wind accretion model and the observed abundances of the sample stars, as well as the uncertainties in the observed abundances.

Table 5 Detailed uncertainties of the abundance analysis for one representative star HD 216219, and the total uncertainties of the abundances for all other sample stars.

	HD 216219 $T_{\rm eff}=5553$ $\log g=3.64$ [Fe/H] $=-0.34$ $\xi_t=1.4$						
		$\sigma_{\rm EW}$	$\Delta T_{\rm eff}$ +100K	$\Delta\log g$ +0.2	Δ[Fe/H] +0.1	$\Delta\xi_t$ +0.2	$\sigma_{\rm tot}$
Δ[Fe/H]$_{\rm I}$		0.07	0.08	−0.01	0.00	−0.04	0.11
Δ[Fe/H]$_{\rm II}$		0.06	−0.03	0.08	0.03	−0.04	0.12
Δ[Na/Fe]		0.04	0.06	0.00	0.00	0.00	0.07
Δ[Mg/Fe]		0.07	0.07	−0.06	0.01	−0.03	0.12
Δ[Al/Fe]		0.03	0.04	−0.02	−0.01	−0.01	0.06
Δ[Si/Fe]		0.05	0.03	0.00	0.00	−0.02	0.06
Δ[Ca/Fe]		0.08	0.08	−0.04	0.00	−0.06	0.13
Δ[Sc/Fe]		0.09	0.01	0.06	0.02	−0.07	0.13
Δ[Ti/Fe]		0.04	0.10	−0.01	−0.01	−0.02	0.11
Δ[V/Fe]		0.04	0.11	−0.01	−0.01	−0.02	0.12
Δ[Cr/Fe]		0.04	0.07	−0.01	−0.01	−0.02	0.08
Δ[Mn/Fe]		0.07	0.09	−0.02	0.00	−0.05	0.13
Δ[Ni/Fe]		0.06	0.08	−0.01	0.00	−0.04	0.11
Δ[Zr/Fe]		0.04	0.13	0.00	0.00	0.00	0.14
Δ[Ba/Fe]		0.06	0.04	−0.02	0.04	−0.05	0.10
Δ[La/Fe]		0.04	0.03	0.08	0.04	−0.03	0.11
Δ[Eu/Fe]		0.03	0.00	0.08	0.02	−0.02	0.09
$\sigma_{\rm tot}$	4395	180622	201657	201824	210946	211594	223617
Δ[Fe/H]$_{\rm I}$	0.11	0.14	0.10	0.12	0.10	0.11	0.13
Δ[Fe/H]$_{\rm II}$	0.13	0.24	0.22	0.19	0.20	–	0.20
Δ[Na/Fe]	0.08	0.16	0.14	0.10	0.13	0.13	0.14
Δ[Mg/Fe]	0.09	0.16	0.14	0.16	0.12	0.10	0.13
Δ[Al/Fe]	0.07	0.13	0.10	0.09	0.10	0.09	0.10
Δ[Si/Fe]	0.07	0.14	0.12	0.10	0.10	0.11	0.11
Δ[Ca/Fe]	0.15	0.18	0.20	0.21	0.18	0.19	0.20
Δ[Sc/Fe]	0.14	0.22	0.17	0.19	0.17	0.18	0.18
Δ[Ti/Fe]	0.12	0.24	0.21	0.20	0.19	0.22	0.21
Δ[V/Fe]	0.12	0.30	0.23	–	0.22	0.20	0.25
Δ[Cr/Fe]	0.10	0.21	0.15	0.15	0.14	0.14	0.19
Δ[Mn/Fe]	0.14	0.20	0.19	0.24	0.21	0.19	0.20
Δ[Ni/Fe]	0.11	0.17	0.14	0.19	0.13	0.15	0.15
Δ[Y/Fe]	0.12	0.26	0.24	0.22	0.17	0.23	–
Δ[Zr/Fe]	0.13	0.25	0.25	0.26	0.19	0.22	0.24
Δ[Ba/Fe]	0.16	0.17	0.09	0.09	0.13	0.13	0.11
Δ[La/Fe]	–	0.17	0.20	0.21	0.13	0.18	0.17
Δ[Eu/Fe]	0.11	0.15	0.10	0.14	0.11	0.12	0.11

In the figure, the variable "a" represents the multiple of the corresponding standard neutron exposure in the ^{13}C profile in the AGB progenitor companion suggested by Gallino et al. (1998) and the higher a value reflects the higher neutron exposure which occurred in the interiors of the AGB progenitor. P refers to the orbital period of the sample star.

There is good agreement between our observed abundances and the theoretical ones for the sample stars. These mean that wind accretion can be the formation scenario of these Ba stars in binary systems.

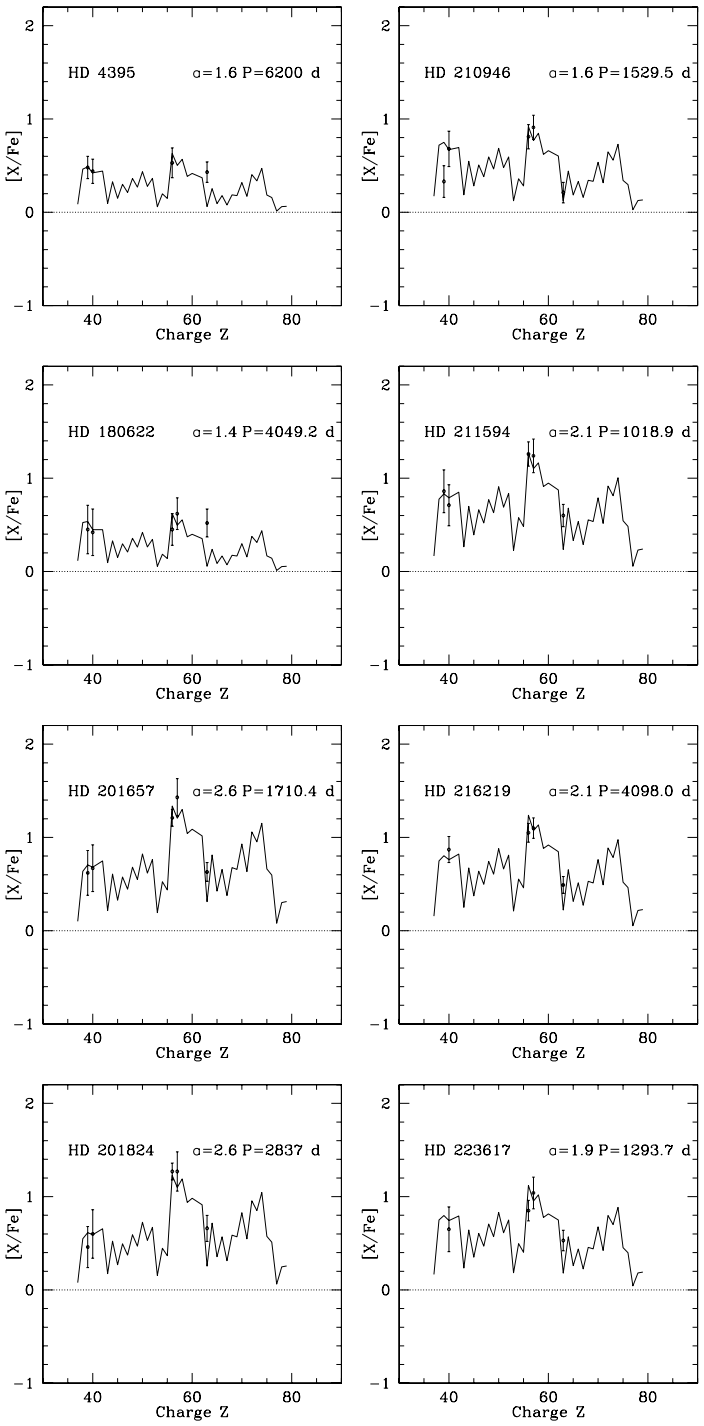

Fig. 6 Fitting of the theoretical to observed heavy-element abundances of sample stars with the standard case of wind accretion. Label "α" represents the durations of the corresponding standard neutron exposures in the ^{13}C profile in the AGB progenitor suggested by Gallino et al. (1998). P refers to the orbital period of the sample star.

Table 6 Orbital Elements of the Sample Stars Derived from Literatures

HD	P (d)	e	Classes	Reference
4395	6200	0.65	–	Preston & Sneden (2001)
180622	4049.2	0.06	mild	Jorissen et al. (1998)
201657	1710.4	0.17	strong	Jorissen et al. (1998)
201824	2837	0.34	strong	Jorissen et al. (1998)
210946	1529.5	0.13	mild	Jorissen et al. (1998)
211594	1018.9	0.06	strong	Jorissen et al. (1998)
216219	4098.0	0.10	mild	Jorissen et al. (1998)
223617	1293.7	0.06	mild	Jorissen et al. (1998)

These are consistent with the suggestions of Jorissen et al. (1998), Zhang et al. (1999) and Liang et al. (2000), who mentioned that Ba stars with periods longer than 1500 or 1600 d could be formed through wind accretion. We should notice that the heavy element abundance patterns of two sample stars with $P > 1000$ d, HD 211594 and HD 223617, can also be explained by wind accretion. Figure 6 also shows that the strong Ba stars generally require higher "a" values in the model than the mild Ba stars, i.e., stronger neutron exposure occurred in the AGB progenitors in their s-process nucleosynthesis.

7 DISCUSSION AND CONCLUSIONS

The chemical compositions of six Ba stars and two CH subgiant stars were obtained with high S/N ratio and high resolution spectra observed by using the 2.16 m telescope at NAOC/Xinglong station. Their stellar atmospheric parameters were determined from reliable methods, and show ranges of $4284 < T_{\rm eff} < 5553$, $1.67 < \log g < 3.64$, $-0.40 <$ [Fe/H] < 0.21, and $1.3 < \xi_t < 1.7$. The model atmospheres were generated by using ATLAS9 code and the updated atomic data of the selected spectral lines for measuring EWs.

We then obtain the abundances of chemical elements, Na, Mg, Al, Si, Ca, Sc, Ti, V, Cr, Mn, Ni, Y, Zr, Ba, La and Eu for our eight sample stars. The elements from Na to Ni, such as α and iron peak elements, show comparable abundances to the Sun, associated with the [Fe/H] in a range of -0.40 to 0.21, which means these Ba stars belong to the Galactic disk. The neutron capture process elements Y, Zr, Ba, La and Eu show obvious overabundances compared with the solar abundances; for example, their [Ba/Fe] values are from 0.45 to 1.27. The abundance patterns of our sample stars are consistent with those obtained for other Ba stars in Začs (1994), Liang et al. (2003) and Smiljanic et al. (2007). Our study enlarges the sample of Ba stars with known chemical abundances. In addition, we further check the formation scenario of these sample stars through a theoretical wind accretion model.

We adopt the angular momentum conservation model of wind accretion to calculate the chemical abundances of Ba stars in the binary systems. The predicted results by the model can explain the observed abundance patterns of the s-process elements well. The abundance patterns of two sample stars, HD 211594 and HD 223617, can also be explained by the wind accretion model, although their orbital periods are 1018.9 and 1293.7 d respectively, which are lower than the low limit of wind accretion formation of Ba stars suggested by Jorissen et al. (1998), 1500 d, and Zhang et al. (1999), Liang et al. (2000), 1600 d. This result could further decrease such a low limit to be about 1000 d.

The masses of the sample stars are also determined and given in Table 3, as well as their errors. For most of them, their masses (0.78–1.92 $M_\odot$) are close to the average masses of typical mild and strong Ba stars given in Jorissen et al. (1998) (their table 9), who suggested that the average mass of typical mild Ba stars is 1.9 or 2.3 $M_\odot$ with the 0.60 or 0.67 $M_\odot$ companion white dwarfs, and the average mass of typical strong Ba stars is 1.5 or 1.9 $M_\odot$ with the 0.60 or 0.67 $M_\odot$ companion white dwarfs. However, the very high mass (4.58 $M_\odot$) of HD 201824 should not be real and the reason could be the large error of its parallax, up to 3 times (1.56/0.56) uncertainty, which will cause the uncertainties of $\sim$0.4 dex in $\log g$ and 3.2 $M_\odot$ in mass. This 0.4 dex uncertainty in $\log g$ is larger than the general case (0.2 dex) of

the sample stars, but will not affect the abundances much. In Table 5 and Figure 6, we adopt the general uncertainties of $\log g$, 0.2 dex, to estimate the uncertainties of abundances for HD 201824.

The derived abundances of our sample stars confirm their "strong" or "mild" Ba star properties well. As shown in Table 4, Figures 3 and 6, for the four mild Ba stars, namely, HD 180622, HD 210946, HD 216219 and HD 223617, their average abundances of s-process elements are [Ba/Fe]$= 0.79$, [La/Fe]$= 0.92$, [Y/Fe]$= 0.43$, [Zr/Fe]$= 0.66$ and [Eu/Fe]$= 0.44$; and for the three strong Ba stars, HD 201657, HD 201824 and HD 211594, their average abundances of s-process elements are [Ba/Fe]$= 1.25$, [La/Fe]$= 1.31$, [Y/Fe]$= 0.65$, [Zr/Fe]$= 0.66$ and [Eu/Fe]$= 0.63$. These show that the s-process element abundances of strong Ba stars are about 0.4 dex (or 0.2 dex) higher than those of the mild Ba stars. However, there are no obvious trends to show that the strong and mild Ba stars have different ranges in metallicity (also see Smiljanic et al. (2007)). Also, there are no obvious indications to show that the orbital periods of mild Ba stars are longer than those of the strong Ba stars.

HD 4395 is a CH subgiant star. HD 216219 has also been classified as a CH subgiant (Smith et al. 1993 and the reference therein) or a mild Ba star (Jorissen et al. 1998; Lü et al. 1991). The CH subgiant was first discovered by Bond (1974). As Luck & Bond (1982) discussed, some of their CH subgiants might more properly be called subgiant barium stars or even main-sequence barium stars. We did not find obvious differences in the abundance patterns of our CH subgiant sample stars and the Ba sample stars, except HD 4395, which shows relatively lower overabundances in its s-process elements. Moreover, the wind accretion models for a binary system can explain the observed overabundances of s-process elements in the CH subgiant stars well, which is the same for other Ba stars. However, our results are not enough to check the suggested evolutionary relation between CH subgiants and classical Ba stars, which will need C/O and Li abundances (Smith et al. 1993; Lambert et al. 1993).

Acknowledgements We thank our referee for very valuable comments which helped us to improve this work a lot. We would like to thank Prof. Gang Zhao, Yuqin Chen, Jianrong Shi, Yujuan Liu, Shu Liu, Kefeng Tan and the *Stellar Abundance and Galactic Evolution Group* at NAOC for sharing their programs for abundance analysis and the helpful discussions about data reduction and abundance analysis. This work was supported by the National Natural Science Foundation of China (NSFC) under Nos. 10403006, 10433010, 10673002, 10573022, 10333060 and 10821061, the National Basic Research Program of China (973 Program) Nos. 2007CB815404, 2007CB815406, 2009CB824800, the Knowledge Innovation Program of the Chinese Academy of Sciences and the Young Researcher Grant of National Astronomical Observatories, Chinese Academy of Sciences.

References

Alonso, S., Arribas, S., & Martínez-Roger, C. 1999, A&AS, 140, 261
Alonso, S., Arribas, S., & Martínez-Roger, C. 2001, A&A, 376, 1039
Bard, A., & Kock, M. 1994, A&A, 282, 1014
Bidelman, W. K., & Keenan, P. C. 1951, ApJ, 114, 473
Biémont, E., Grevesse, N., Hannaford, P., & Lowe, R. M. 1981, ApJ, 248, 867
Biémont, E., Karner, C., Meyer, G., et al. 1982, A&A, 107, 166
Boffin, H. M. J., & Jorissen, A. 1988, A&A, 205, 155
Boffin, H. M. J., & Začs, L. 1994, A&A, 291, 811
Bond, H. E. 1974, ApJ, 194, 95
Burbidge, E. M., Burbidge, G. R., Fowler, W. A., & Hoyle, F. 1957, Rev. Mod. Phys., 29, 547
Carquillat, J. M., Jorissen, A., Udry, S., & Ginestet, N. 1998, AAS, 131, 49
Chen, Y. Q., Nissen, P. E., Zhao, G., et al. 2000a, in The Galactic Halo: From Globular Cluster to Field Stars, Proceedings of the 35th Liege International Astrophysics Colloquium, eds., A. Noels, P. Magain, D. Caro, et al., Belgium: Institut d'Astrophysique et de Geophysique, 35, 219
Chen, Y. Q., Nissen, P. E., Zhao, G., Zhang, H. W., & Benoni, T. 2000b, A&AS, 141, 491
ESA 1997, the Hipparcos and Tycho Catalogues, ESA SP-1200
Fuhr, J. R., Martin, G. A., & Wiese, W. L. 1988, JPCRD, 17, Suppl.4

Gallino, R., Arlandini, C., Busso, M., et al. 1998, ApJ, 497, 388
Gómez, A. E., Luri, X., Grenier, S., et al. 1997, A&A, 319, 881
Grevesse, N., & Sauval, A. J. 1998, Space Sci. Rev., 85, 161
Griffin, R. F. 1980, MNRAS, 193, 957
Han, Z. W., Eggleton, P. P., Podsiadlowski, P., & Tout, C. A. 1995, MNRAS, 277, 1443
Hannaford, P., Lowe, R. M., Grevesse, N., Biemont, E., & Whaling, W. 1982, ApJ, 261, 736
Jorissen, A., & Mayor, M. 1988, A&A, 198, 187
Jorissen, A., Van Eck, S., Mayor, & M., Udry, S. 1998, A&A, 332, 877
Krishnaswamy, K., & Sneden, C. 1985, PASP, 97, 407
Kurucz, R. L. 1993, CD-ROM, 13, Smithsonian Astrophysics Observatory, Cambridge
Lambert, D. L., & Warner, B. 1968, MNRAS, 139, 115
Lambert, D. L., Smith, V. V., & Heath, J. 1993, PASP, 105, 568
Lambert, D. L., Health, J. H., Lemke, M., et al. 1996, ApJS, 103, 183
Liang, Y. C., Zhao, G., & Zhang, B. 2000, A&A, 363, 555
Liang, Y. C., Zhao, G., Chen, Y. Q., Qiu, H. M., & Zhang, B. 2003, A&A, 397, 257
Liu, J. H., Zhang, B., Liang, Y. C., & Peng, Q. H. 2000, A&A, 363, 660
Luck, R. E., & Bond, H. E. 1982, ApJ, 259, 792
Luck, R. E., & Bond, H. E. 1991, ApJS, 77, 515
Lü Phillip, K. 1991, AJ, 101, 2229
McClure, R. D., Fletcher, J. M., & Nemec, J. M. 1980, ApJ, 238, L35
McClure, R. D 1983, ApJ, 268, 264
McClure, R. D., & Woodsworth, A. W. 1990, ApJ, 352, 709
Mennessier, M. O., Luri, X., Figueras, F., et al. 1997, A&A, 326, 722
Nissen, P. E., Chen, Y. Q., Schuster, W. J., & Zhao, G. 2000, A&A, 353, 722
O'Brian, T. R., Wickliffe, M. E., Lawler, J. E., et al. 1991, JOSAB, 8, 1185
Preston, G. W., & Sneden, C. 2001, AJ, 122, 1545
Smith, V. V., Coleman, H., & Lambert, D. 1993, MNRAS, 417, 287
Smiljanic, R., Porto de Mello, G. F., & da Silva, L. 2007, A&A, 468, 679
Sneden, C. 1983, PASP, 95, 745
Udry, S., Jorissen, A., Mayor, M., & Van Eck, S. 1998a, A&AS, 131, 25
Udry, S., Mayor, M., Van Eck, S., et al. 1998b, A&AS, 131, 43
Weise, W. L., & Martin, G. A. 1980, NSDRS-NBS, 68
Yi, S. K., Kim, Y. C., & Demarque, P. 2003, ApJS, 144, 259
Začs, L. 1994, A&A, 283, 937
Zhang, B., Liu, J. H., Liang, Y. C., & Peng, Q. H. 1999, Chin. Astron. Astrophys., 23, 189
Zhao, G., Qiu, H. M., Chen, Y. Q., & Li, Z. W. 2000, ApJ, 126 ,461